

# Towards interpreting the origin of the APTw contrast in the human brain using a physically interpretable machine learning model

Florian Kroh<sup>1</sup>, Philip S. Boyd<sup>1</sup>, Nikolaus von Knebel Doeberitz<sup>1</sup>, Mark E. Ladd<sup>1</sup>, Daniel Paech<sup>1</sup>, Andreas Korzowski<sup>1</sup>  
<sup>1</sup> German Cancer Research Center (DKFZ), Heidelberg, Germany

**INTRODUCTION:** The amide proton transfer-weighted (APTw) contrast represents a valuable imaging biomarker for clinical assessment of gliomas. However, the underlying molecular origins of the APTw contrast in vivo are still debatable. This work aims to expand the current knowledge about the APTw contrast mechanisms in the human brain at  $B_0 = 3$  T by developing a physically interpretable model (PIM) enabling the calculation of APTw contrast values based on the interpretable  $MTR_{Rex}$  contrasts.

**METHODS:** All data used in this work was acquired as part of a clinical study including a total of 146 glioma patients using a 3T whole-body MR scanner (Siemens; MAGNETOM Prisma). The CEST-related sequences used in this work are (i) two low-power CEST scans ( $B_1=0.6$  and  $0.9 \mu T$  [1]), (ii) an APTw CEST scan ( $B_1=2\mu T$  [2]), (iii) a WASABI scan [3], and (iv) a saturation recovery T1 measurement. All scans are based on the 3D-Snapshot-CEST-Sequence [4]. The two low-power CEST scans were used to calculate the  $B_1$  corrected interpretable  $MTR_{Rex}$  contrasts for the amide, rNOE and ssMT pools (see [1]). Using these contrasts, a machine learning model was created to enable the APTw contrast calculation in an interpretable manner. The model was constructed by using multiple linear regression (LR) models that were each created for a distinct range of  $B_1$  and  $T_1$  values with the aim to account for

$B_1$  and  $T_1$  dependencies for the different contributions. The APTw contrast for each voxel  $n$  can ultimately be represented based on the  $MTR_{Rex}$  values ( $x_i$ ),  $B_1$ , and  $T_1$  via eq. (1). The sensitivity in eq. (1) is the change of the predicted APTw contrast value by one standard deviation change of the corresponding input feature and is therefore the relevant parameter, describing the change in contribution to APTw contrast for a specific physical situation (i.e.  $B_1, T_1$ ).

$$APTw_n(B_1, T_1) = \overline{APTw}_{train}(B_1, T_1) + \sum_{i=1}^3 \frac{x_{n,i} - \bar{x}_{i,train}(B_1, T_1)}{SD(x_{i,train}(B_1, T_1))} * Sens.Std.x_i(B_1, T_1) \quad (1)$$

Parameters with subset **train** describe the contrasts mean or standard deviation based on all training voxels

**RESULTS:** Representative results in Figure 1 show a good match between ground truth and APTw contrast predicted with the PIM, especially in the tumor region. This is confirmed by the overall mean absolute error of 0.92 %. Figure 2 shows the extracted sensitivity maps (whole cohort) indicating a strong change of amide, rNOE and ssMT contribution to the APTw contrast depending on the  $T_1$  and  $B_1$  values. Especially for the amide and rNOE an absolute increase of sensitivity can be observed towards low  $B_1$  and high  $T_1$  values.

**DISCUSSION:** This PIM enabled the successful translation of interpretable CEST signals into contribution to their respective APTw contrasts not only as a black-box model but by explicitly exploiting physically relevant information. This novel approach allowed not merely (i) the identification of the isolated amide and rNOE contrasts as the dominating influences on the APTw contrast, in coherence with literature. But, more interestingly, (ii) this PIM also revealed significant dependencies of amide and rNOE contributions on changes in the controllable  $B_1$  and tissue-specific  $T_1$ .

**CONCLUSION:** Ultimately, the PIM allowed the identification of amide- and rNOE-driven sensitivity regimes of the APTw contrast, enabling an enhanced biophysical understanding of the CEST phenomenon in vivo, thus potentially improving the clinical assessment of gliomas using the APTw contrast.

**REFERENCES:** 1. Goerke S, *et al.* Magn Reson Med. 2019;82:622-632 2. Zhou J, *et al.* J Magn Reson Imaging. 2019;50(2):347-64 3. Schuenke P, *et al.* Magn Reson Med. 2017;77:571-580 4. Deshmene A, *et al.* Magn Reson Med. 2019;81(4):2412-23

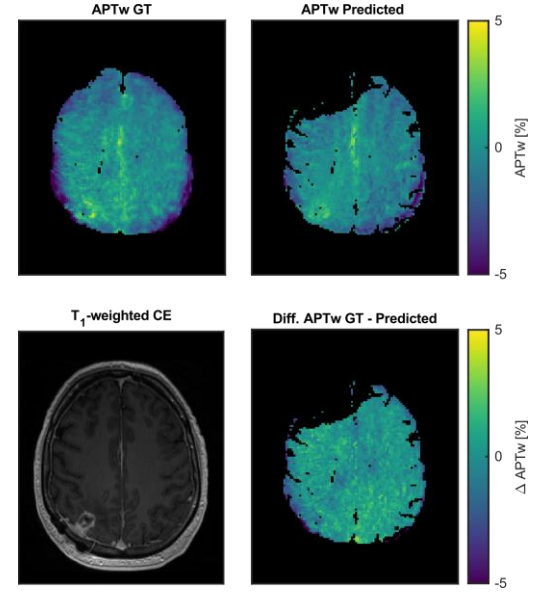


**Fig.1:** The voxel wise predicted APTw contrast using the PIM for a representative subject and slice is displayed. Additionally, a T1-weighted CE map, the acquired APTw ground truth image and a difference map are shown. Note that the prediction is masked by specific quality criteria.

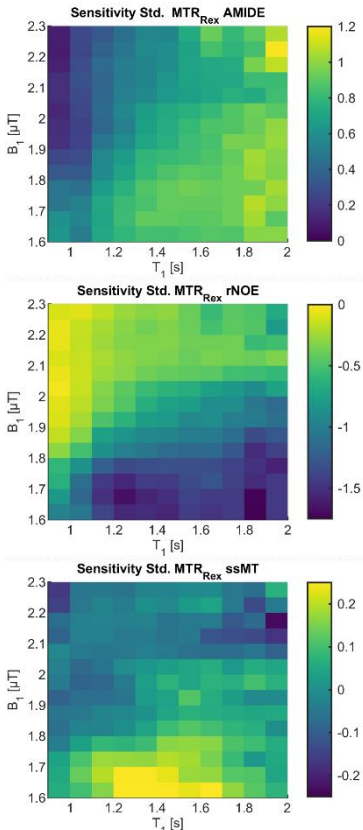


**Fig. 2:** The sensitivities for  $MTR_{Rex}$  AMIDE (top), rNOE (middle), and ssMT (bottom) contributions as determined for each  $B_1$ - $T_1$  bin by an individual LR model. Note the different scales for each contrast.